Received July 17, 2020; revised October 4, 2020; accepted October 11, 2020. Date of publication 14 October 2020; date of current version 3 November 2020.
The review of this article was arranged by Editor C. C. McAndrew.

Digital Object Identifier 10.1109/JEDS.2020.3030880

Ionization Damage Effects of Pulse Discharge Circuit Switched by Anode-Short MOS-Controlled Thyristor

LEI LI [1,2] (Member, IEEE), ZE-HONG LI [2] (Senior Member, IEEE), JIN-PING ZHANG [2] (Member, IEEE), YU-ZHOU WU [2], XIAO-CHI CHEN [1], MIN-REN [2] (Member, IEEE), BO ZHANG [1] (Senior Member, IEEE), AND YUAN JIAN [1]

1 Institute of Nuclear Physics and Chemistry, Chinese Academy of Engineering Physics, Mianyang 621000, China
2 State Key Laboratory of Electronic Thin Films and Integrated Devices, University of Electronic Science and Technology of China, Chengdu 610000, China

CORRESPONDING AUTHOR: L. LI and Z. H. LI (e-mail: skyhappier@163.com; lizh@uestc.edu.cn)

ABSTRACT The MOS-controlled Thyristor (MCT) has been characterized by MOS-gating, high current rise rate, and high blocking capabilities. The anode short MCT (AS-MCT) is distinguished from the conventional MCT by an anode-short structure, which forms an extracting path for the leakage current at the gate-ground and develops a normally-off characteristic. The AS-MCTs are ideal switches for pulse discharge application. As a composite structure made of metal-oxide-silicon and bipolar junction transistors, AS-MCT is susceptible to ionization damage. This work reports the experimental results for the degradation of zero-load (or short) pulse discharge circuit characteristics induced by the ionization damage of its AS-MCT switch following cobalt-60 γ-ray dose up to 9160 Gy(SiO_2). The radiation-induced leakage current in AS-MCT accounts for the degradations of charging time and peak surging current of the pulse discharge circuit. These degradations show a "tick"-like dependence on the γ-ray dose which are recoverable after high dose exposures, thousands of Gy(SiO_2). From device and circuit physics perspectives, the damages on pulse discharge circuit are modelled, and then, this article proposes, the mechanism behind the characteristics degradation of pulse discharge circuit from the total ionization dose damage of AS-MCT switch.

INDEX TERMS Total ionization dose damage, anode-short MOS-controlled thyristor, pulse discharge circuit, surge current.

I. INTRODUCTION

Pulse discharge technology based on the capacitive energy storage has been extensively utilized in several applications such as exciter lasers, particle accelerators and electromagnetic launchers, slapper detonator and so on [1]–[6]. In a pulse discharge circuit (PDC), as presented in Fig. 1, the energy stored in high voltage capacitor should be released as fast and efficient as possible to produce surge current of high peak, several kA, and high rise rate, $kA\cdot\mu s^{-1}$. Thereafter, the electric energy is transferred to the loads (e.g., resistor and inductor) via the surge current within hundreds of nanoseconds [4]–[6], which can effectuate the subsequent actions of the loads (e.g., the explosion of metal foil in detonator). MOS-trolled Thyristor (MCT) is the natural switching unit for PDCs owing to the surge in the current capability without current saturation, but with a high current density up to $kA\cdot cm^{-2}$ and a high current rising rate of $\sim 10^2$ $kA\cdot\mu s^{-1}$, besides Metal-Oxide-Silicon (MOS) gating [4], [7]. A conventional MCT structure requires a gate voltage to form OFF-FET channel extracting carriers, and henceforth realizing a high blocking capability, which complicates the driver circuit. The anode-short MCT (AS-MCT), proposed over the last ten years [1], [8], features a normally-off characteristic owing to the introduction of an anode-short structure as presented in Fig. 2. The AS-MCT is a potential alternative to conventional MCT for pulse power applications.

This work is licensed under a Creative Commons Attribution 4.0 License. For more information, see https://creativecommons.org/licenses/by/4.0/

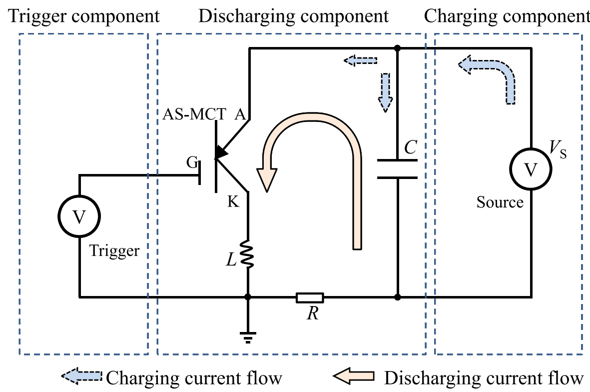

FIGURE 1. Illustration of pulse discharge circuit switched by AS-MCT.

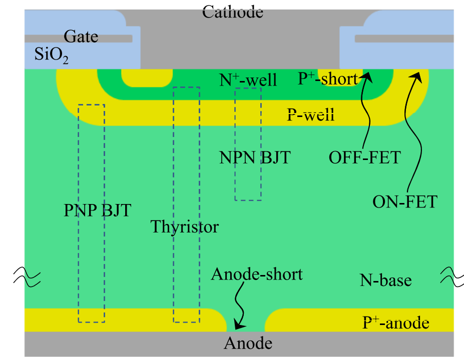

FIGURE 2. Cross-section of N-base AS-MCT chip [1].

In radiation environments, e.g., space mission, the PDCs suffer from the total ionization dose (TID) induced by energetic radiation, such as γ-rays, protons and electrons [9]–[16]. After TID exposures, the dominant defects are the oxide charges (positively charged oxygen vacancy) within SiO_2 and interfacial traps (silicon dangling bond) near/at SiO_2-Si interface. The charge state of interfacial traps depends on the location of substrate fermi energy level, which can be positively and negatively charged for N-type and P-type substrate respectively. The two charged defects can alter the substrate surface potential. And, the interfacial traps can act as effective recombination centres for neutral substrate or generation centres for depletion region. The changes of devices electrical characteristics following ionization exposures are results from the synergical effects of the electrostatic and recombination/generation phenomenons. The typical TID damages on MOS contain shifts of turn-on and turn-off voltages, degradation of subthreshold swing, and increase of off-state leakage current [12]. For Bipolar-Junction-Transistors (BJTs), the increase of base leakage current and degradation of dc current gain are the dominant damage effects [13], [14]. As a semiconduction with composite structure made of MOS and BJTs, MCTs are sensitive to TID damage. The earlier work in 1989 reports the TID damage on the P-type conventional MCTs [17]. The gate voltages required to turn the conventional MCTs on and off shift following TID exposures. The AS-MCT, a novel power switch, has been fabricated over the last ten years.

Recently, we have experimentally studied the TID damage on the N-type AS-MCTs induced by cobalt-60 γ-rays [2]. It indicates that the AS-MCT is sensitive to ionization damage. For an un-irradiated AS-MCT, the leakage current at an anode voltage of 1000 V is on the order of ∼0.1 μA. The leakage current can amplify by three orders of magnitude to ∼0.1 mA following γ-ray exposures up to thousands of Gy(SiO_2). For the case of low energy PDC, such as slapper detonator [6], the voltage of charging source is typically in the range of 1000 to 3000 V, and its output power is usually on the order of 0.1-1 W [4], [18]. After γ-ray exposures, the power consumption in AS-MCT is comparable with the output power of charging source. Thus, we can reasonably speculate that the electrical properties of PDC switched by AS-MCT can be sensitive to TID. And, it is of importance to study the TID responses of PDCs prior to their applications in radiation environments.

This work reports the experimental results for the degradation of PDC characteristics induced by the TID damage on its AS-MCT switch, including the charge and discharge behaviours. We also propose the mechanism for the TID-induced degradation of the PDC characteristics from the prospectives of circuit and device physics. The loads of PDCs vary with applications, which can be resistors (e.g., bridge foil in detonator) and inductors (e.g., motor in machine) [5]. For the purpose of generality, we focus on the case of short PDC, i.e., no loads in PDC besides the parasitic resistor and inductor as presented in Fig. 1. A short PDC represents an ideal pulse discharging circuit which can produce a surge current of maximum peak, and is suitable to describing the energy transfer ability of pulse discharging system. The AS-MCT can be classified according to the type of ON-FET. In N-type AS-MCT, an N-tpye ON-FET turns on the device. As the switching delay of N-type AS-MCTs is short (∼100 ns) due to the high electron mobility, these devices are favorable for high speed applications. Thus, this work focus on TID effect of N-type AS-MCTs switched PDCs.

II. BACKGROUND

An AS-MCT is comprised of thousands of cells, and each cell is a composite structure of MOS and BJTs as shown in Fig. 2. The N-base and P-well serve as the common regions for the upper N^+-well/P-well/N-base (NPN) and lower P-well/N-base/P^+-anode (PNP) BJTs. The trigger-on of AS-MCT denotes the latch-up of vertical N^+-well/P-well/N-base/P^+-anode (PNPN) thyristor structure, i.e., the coupling of the two BJTs. The AS-MCT features a normally-off characteristic (zero gate anode voltage) owing to the introduction of anode-short structure which suppresses the current gain of lower PNP. Under such conditions, the AS-MCTs can be operated in the forward blocking mode, and the upper NPN with wide collector region (N-base) is capable of supporting the high anode voltage. Once the gate

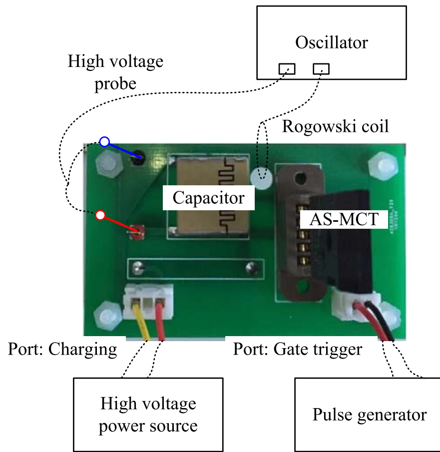

FIGURE 3. Photo of pulse discharge circuit test board.

voltage exceeds a critical value (~0.7 V), the electrons flow from the N^+-well into the N-base region which effectuate the hole injection from P^+-anode/N-base junction. This sets up the coupling of PNP and NPN BJTs, which turns on the latch-up of vertical thyristor in the AS-MCT structure, to support an ultra-high current density and low on-resistance. A detailed description for the device physics of AS-MCT can be found in [1].

A PDC usually contains three components as presented in Fig. 1. During a complete discharging process, the PDC goes through two stages, including charging and discharging ones. In the charging stage, the high voltage capacitor is charged by the charging component. Under such conditions, the AS-MCT is operated in the forward blocking mode. Once the AS-MST is triggered on by a gate voltage pulse produced by the trigger component, the PDC enters the discharging stage. Thereafter, the electric energy stored in capacitor is released, which produces a surge current within the discharge component.

III. EXPERIMENTAL DETAILS

A. PULSE DISCHARGE CIRCUIT

A test PDC was fabricated on a PCB board as illustrated in Fig. 3. The voltage on capacitor and the surge current were monitored by Tek P5205A differential high voltage probe and CWT HF60B Rogowski coil respectively. Both the transient voltage and current signals were recorded by Tek DPO70804C high speed oscillator.

In the charge stage, the capacitor was charge by SRS PS350 power source which acted as the charging component of PDC. In the discharge stage, a trigger voltage pulse was produced by Agilent 33220A signal generator, acting as the trigger component of PDC, to ignite the AS-MCT switch. The trigger pulse is of 0 V bench-mark, 5 V amplitude, and 10 μs width. The AS-MCT enters on-state mode from blocking one after a short delay, ~0.1 μs, once the trigger voltage is larger than the threshold voltage of AS-MCT, ~0.7 V. As the delay time is much shorter than the discharge time, several μs, we can omit the transition state and assume an ideal switch-on for AS-MCT.

TABLE 1. Parameters for pulse discharge circuits.

Parameter	Value	Note
Capacitance of high voltage capacitor (C)	0.368 μF	–
Parasitic inductance (L)	29 nH	–
Parasitic resistance (R)	39 mΩ	–
Probe resistance (R_P)	5 MΩ	–
Power limitation of power source (P)	0.29 W	–
Voltage limitation of power source (V_L)	1000 V	–
Current limitation of power source (I_L)	0.3 mA	–
Time (t)	–	–
Output voltage of power source (V_S)	–	–
Output current of power source (I_S)	–	–
Voltage on high voltage capacitor (V_C)	–	Charge stage
Charging time for capacitor (t_c)	–	Charge stage
Leakage current of AS-MCT in forward blocking mode (I_{MCT})	–	Charge stage
Equivalent resistance of AS-MCT in forward blocking mode (R_{MCT})	–	Charge stage
Effective resistance of charging circuit component of PDC (R_{eff})	–	Charge stage
V_C at the beginning of discharge (V_{C0})	–	Discharge stage
Voltage on parasitic inductance (V_L)	–	Discharge stage
Voltage on parasitic resistance (V_R)	–	Discharge stage
Surging current (I_D)	–	Discharge stage
Peak value of I_D (I_{peak})	–	Discharge stage

For clarity, we define the terms and variables for PDCs used in the following sections which are listed in Table 1. As stated in Section I, we focus on the low energy PDCs. In such cases, capacitance (C), power limitation (P) and voltage limitation (V_L) are typically on the order of 0.1 μF, 0.1 W and 1000 V respectively [4], [18]. The parameters of our test PDC are listed in Table 1.

B. AS-MCT AND γ-RAY IRRADIATION

The AS-MCTs used in this work have been fabricated with the commercial IGBT process [1], [3]. Fig. 2 presents the cell unit of AS-MCT. The cell unit is with the size of 20 μm (Width)×625 μm (Thickness), and a chip contains 1.3×10^5 cell units. A single die is mounted on a TO-247 plastic package. The fabricated devices show a forward blocking capability of ~1800 V at the gate-ground and a static forward voltage drop of 1.5 V at an anode current of 12 A. The sample details can be founded in [1].

Several devices from the single diffusion lots have been irradiated by cobalt-60 source in the Institute of Nuclear Physics and Chemistry [13]. All pins of the samples were shorted and grounded during irradiation. The dose rate was 3.2×10^{-2} Gy(SiO_2)·s^{-1}, and the accumulated dose on the samples was up to 9160 Gy(SiO_2). The forward conductive and blocking current-voltage curves of AS-MCT were measured by Keithley 2600-PCT power device curve tracer. During the tests for conductive characteristics, the gate voltage was fixed at 5 V, which is far larger than the threshold voltage of AS-MCT. When we measured the blocking characteristics, the gate was zero biased. Both irradiations and measurements were performed at room temperatures.

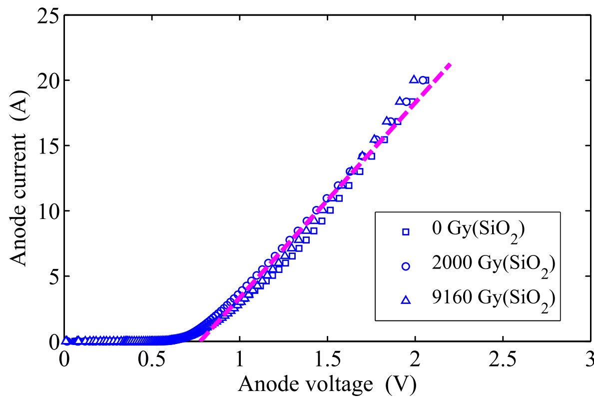

FIGURE 4. Forward anode current-voltage curves of AS-MCT before and after γ-ray exposures (the data are extracted from the [2, Fig. 11]). The dash line is linear fitting result for the experimental data of all three dose levels for current in the range of 1 to 20 A, and its correlation coefficient (R^2) is 0.88.

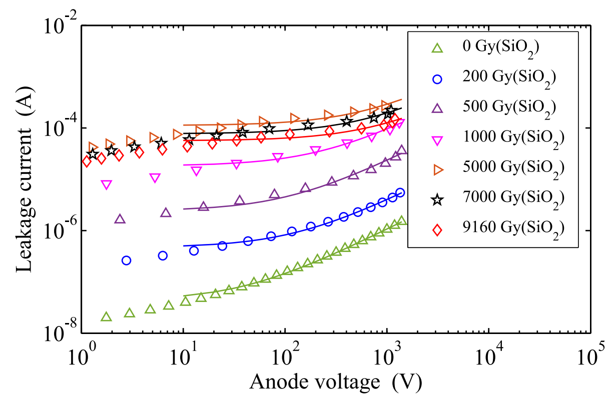

FIGURE 5. Forward blocking characteristics of AS-MCTs before and after γ-ray exposures (the data are extracted from the [2, Fig. 5]). During measurements, the gate electrode is open. The solid lines are linear fitting results for the corresponding dose levels in the range of 10 to 1400 V, and their correlation coefficients (R^2) are in the range of 0.92–0.99. The breakdown voltage of our devices is ∼1800 V. During the test, the maximum anode voltage is limited to 1400 V to avoid the breakdown.

IV. DAMAGE ON AS-MCT SWITCH

A. FORWARD CONDUCTIVE CHARACTERISTICS

Fig. 4 illustrates the forward conductive current-voltage curves of AS-MCTs before and after γ-ray exposures. The conductive characteristics exhibit excellent γ-ray damage tolerance, i.e., the anode current up to ∼20 A is almost unchanged even after high dose irradiation of 9160 Gy(SiO_2).

For AS-MCTs operated in the forward conductive mode, the bulk current flowing though the vertical thyristor structure dominates the anode current, which is naturally immune to the surface ionization damages. After high dose exposures, ∼ 10^4 Gy(SiO_2), the displacement damage induced by the secondary electrons (hundreds of keV) of cobalt-60 γ-ray can be significant for bipolar devices operated in small injection regime. In the conductive mode, the AS-MCT works in high level injection regime, and the carrier concentrations in chips are relatively high. Under such conditions, the Auger mechanism (a band-to-band recombination theory) [19], not the Shockley-Read-Hall mechanism, dominates the carrier recombination behaviours. Our previous displacement damage experiments by neutron have demonstrated this conclusion [1], i.e., the conductive current of AS-MCT is insensitive to displacement damage. Thus, we can reasonably speculate that the conductive behaviours of AS-MCT at very high currents, hundreds of A, are also insensitive to surface and bulk damages induced by cobalt-60 γ-ray. Fig. 4 also indicates that the AS-MCT in conductive mode behaves as a linear resistor. As a result, the MCT can be behaviorally modeled as a resistor (∼65 mΩ) during the capacitor discharge.

B. FORWARD BLOCKING CHARACTERISTICS

Fig. 5 shows the forward blocking current-voltage curves of AS-MCTs before and after γ-ray exposures. The leakage current of AS-MCT (I_{MCT}) mainly contains three components, which are currents from ON-FET channel ($I_{ON\text{-}FET}$), depleted N-base surface region ($I_{N\text{-}base}$) and P^+-anode/N-base junction (I_{PN}) as presented in Fig. 6. For AS-MCT in the forward blocking mode, the ON-FET (N-base/P-well/N^+-well) is operated in subthreshold regime. The positive oxide charges tend to reverse the P-well channel which results in an increase in $I_{ON\text{-}FET}$ like that in N-MOS. The surface region of N-base is depleted when AS-MCT is in the blocking mode. After TID exposures, the interface-trap-induced generation current increases which is amplified by the upper NPN structure. This amplified current leads to the increase of $I_{N\text{-}base}$. Both the increases of $I_{ON\text{-}FET}$ and $I_{N\text{-}base}$ can enhance the hole injection by P^+-anode/N-base junction, which brings about an increase in I_{PN}. Thus, after γ-ray exposures, all the three leakage current components increase. Thereafter, I_{MCT} amplifies by three orders of magnitude from ∼0.01-0.1 μA to ∼0.01-0.1 mA after γ-ray exposures up to ∼5000 Gy(SiO_2). Then, I_{MCT} decreases with a further increase of dose, as the γ-ray induced displacement damage becomes

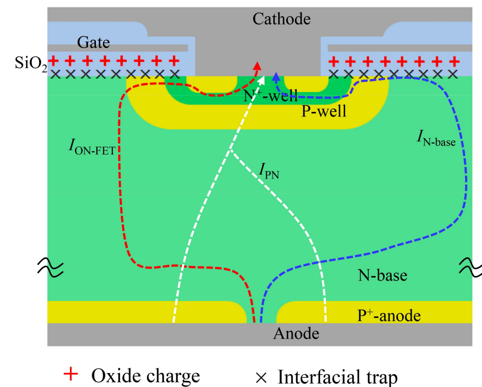

FIGURE 6. Illustration of leakage current in AS-MCT. In figure, the three main components of leakage current are plotted, which are currents from ON-FET channel ($I_{ON\text{-}FET}$), depleted N-base surface region ($I_{N\text{-}base}$) and P^+-anode/N-base junction (I_{PN}).

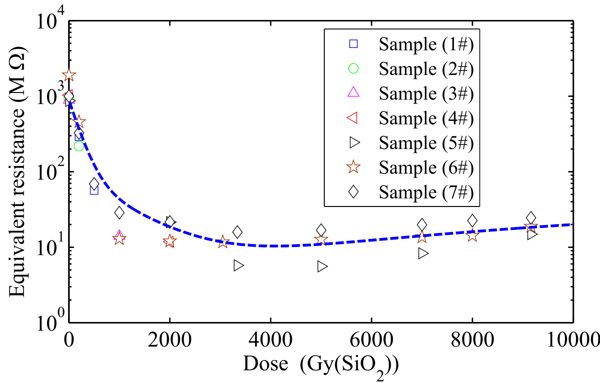

FIGURE 7. Dose dependence of equivalent resistance for AS-MCT operated in the open-gate forward blocking mode. The dash line indicates the trend of resistance following TID exposures.

significant which can suppress the TID damage of $I_{\text{N-base}}$ and I_{PN}.

A precisely modelling for I_{MCT} is complicated and beyond the scope of this work. Fig. 5 also indicates that the current-voltage characteristic of AS-MCT operated in the forward blocking mode approximately behaves as a linear resistor for anode voltage in the range of 10 to 1400 V. As presented in the following Section V, the charge time of PDC is on the order of s. In charge stage, the voltage on AS-MCT (in parallel with capacitor) quickly surpasses tens of Volts within tens of ms. Thereafter, during most of the charging time, the AS-MCT supports a relative high voltage, and thus, can be approximately modelled as a resistor R_{MCT}. R_{MCT} is a differential resistor, which is extracted by the linear curve fitting, as presented in Fig. 5. The damage of R_{MCT} exhibits dose dependence as presented in Fig. 7. For low dose exposures, up to $\sim$4000 Gy(SiO_2), R_{MCT} decreases significantly from $\sim$1000 to $\sim$10 MΩ. Then, R_{MCT} slightly increases with a further increase of dose as the γ-ray induced displacement damage alleviates the increase of leakage current.

V. DAMAGE ON CHARING CHARACTERISTICS

A. EXPERIMENTAL RESULTS

Fig. 8 displays the variations in voltage waves on capacitor (V_{C}) of PDCs in charge stage, before and after the γ-ray irradiation. The damage of V_{C} waves depends on dose. For the case of low dose, $\sim$1000 Gy(SiO_2), the charging time (t_{c}) increases and the capacitor voltage at the end of charge stage (V_{C0}) is almost unchanged. After middle dose exposures, $\sim$3000 Gy(SiO_2), V_{C0} decreases significantly. Then, with a further increase of dose, V_{C0} is restored to its initial state, and the degradation of t_{s} is alleviated.

B. MODELLING

During the charge stage, the AS-MCT switch is operated in the forward blocking mode, and can be behaviorally modelled as a resistor (R_{MCT}) as stated in IV.B. Fig. 9 presents the equivalent circuit for PDC in charging. The capacitor, voltage probe and AS-MCT are in parallel with the power

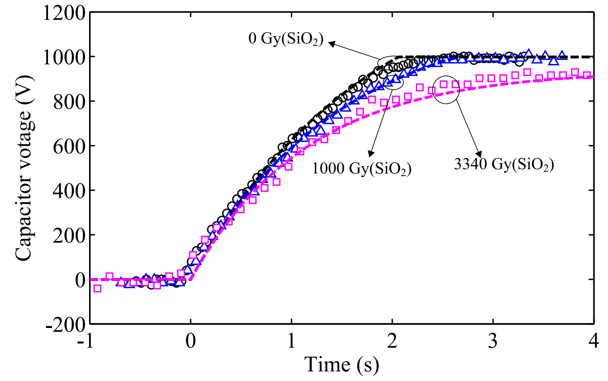

(a) Lower dose

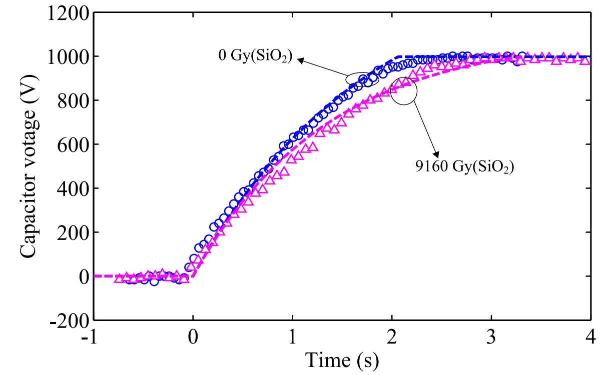

(b) Higher dose

FIGURE 8. Voltage waves on capacitor of PDC in charge state, before and after the γ-ray irradiation. The markers are experimental results, and the dash lines are calculated results by (2) and (6).

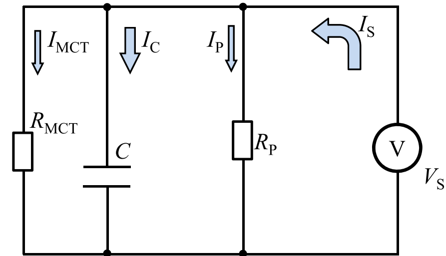

FIGURE 9. Simplified equivalent circuit for PDC in charging.

source. In the charging circuit, the output current (I_{S}) of power source can be expressed as

$$I_{\text{S}} = I_{\text{C}} + I_{\text{P}} + I_{\text{MCT}} = C\frac{\mathrm{d}V_{\text{C}}}{\mathrm{d}t} + \frac{V_{\text{C}}}{R_{\text{P}}} + \frac{V_{\text{C}}}{R_{\text{MCT}}} \quad (1)$$

The parameters are defined in Table 1 (Section III-A). The solution to (1) depends on the operation mode of power source. The power source charges the capacitor with a constant and maximum current until the power limitation (P) is reached, i.e., $I_{\text{S}} = I_{\text{L}}$. Then the capacitor is charged by a constant P until the voltage limitation (V_{L}) of power source is reached.

For the case of constant current I_{S}, the initial condition is V_{C}=0 V. Then, we can figure out the solution to (1) for

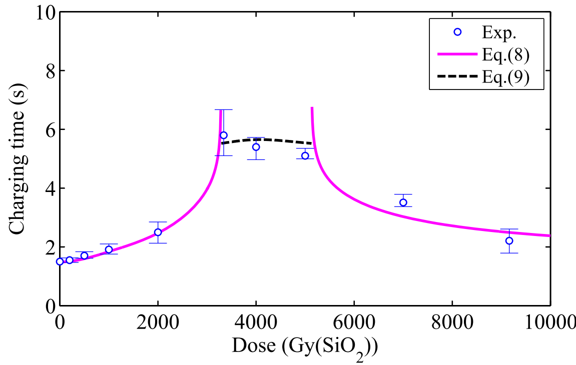

FIGURE 10. Dose dependence of charging time.

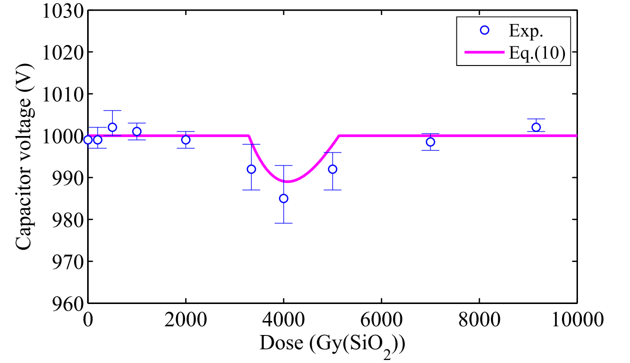

FIGURE 11. Dose dependence of capacitor voltage at the end of charge stage.

such the case, which can be expressed as

$$V_C(t) = I_L R_{eff}\left[1 - \exp\left(-\frac{t}{CR_{eff}}\right)\right] \tag{2}$$

R_{eff}, the effective resistance of AS-MCT R_{MCT} and high voltage probe R_P in parallel, takes the form as

$$R_{eff} = \frac{R_P R_{MCT}}{R_P + R_{MCT}} \tag{3}$$

For the case of constant power, the capacitor is charged by a changing I_S under the constraint of

$$P = V_C I_S \tag{4}$$

With (2) and (4), we can figure out the transition time (t_s) for the change of charging mode from constant current to constant power one, which can be expressed as

$$t_s = R_{eff}C\ln\left(\frac{I_L R_{eff}}{I_L R_{eff} - P/I_L}\right) \tag{5}$$

By substituting (4) into (1), and with the boundary condition in (5), we can obtain the solution to (1) for constant power case, which can be expressed as

$$V_C(t) = \sqrt{R_{eff}C\left[\frac{P}{C} - \exp\left(-\frac{2t + 2t_1}{R_{eff}C}\right)\right]} \tag{6}$$

where t_1 is a simplifier factor which takes the form as

$$t_1 = \frac{-1}{2}R_{eff}C\left[\ln\left(\frac{-P^2}{I_L^2 R_{eff}C} + \frac{P}{C}\right) - \ln\left(\frac{I_L R_{eff}}{I_L R_{eff} - P/I_L}\right)\right] \tag{7}$$

When V_C approaches the limitation voltage of power source (V_L), the source power gradually decreases to zero, i.e., P is time-dependent at the end of charge stage. As the duration time of changing P is short, tens of ms, we omit the changes of P in (6) for simplification, and assume that V_C is unchanged once it equals V_L.

C. DAMAGE MECHANISMS

The equivalent leakage resistance (R_{MCT}) is a donator for the TID damage on AS-MCT in the blocking mode as stated in the previous Section IV-B. R_{MCT} is previously determined in Fig. 7. Then, by substituting the parameters in Table 1 into (2) and (6), we can figure out the voltage waves on capacitor (V_C) as presented in Fig. 8. There is excellent agreement between the experimental data and model for the V_C response of the AS-MCT before and after TID damage.

The charging time (t_c) can be obtained by (6) under the constraint of $V_C = V_L$, which takes the form as

$$t_c = -\frac{R_{eff}C}{2}\ln\left(\frac{R_{eff}P - V_L^2}{R_{eff}C}\right) - t_1 \tag{8}$$

After γ-ray exposures, the leakage current passing though AS-MCT (I_{MCT}) increases which effectuates a decrease in R_{MCT}. For high dose exposures, the degradation of R_{MCT} results in significant decrease in R_{eff} (see (3)). Thereafter, t_c in (8) increases significantly. Equation (6) predicts a maximum V_{C0} with value of $\sqrt{R_{eff}P}$. After high dose exposures, $\sqrt{R_{eff}P}$ decreases significantly, and can be smaller than the expected value of V_{C0}, i.e., the limitation voltage of power source (V_L). Thereafter, V_C can not be charged to V_L, and is just approaching $\sqrt{R_{eff}P}$ with the increasing t, In such cases, (8) is incapable of calculating t_c as t_c is infinite. We define that t_c is the time interval where V_C equals $0.95\sqrt{R_{eff}P}$ to avoid the divergency of t_c. Then, with (6) under the constraint of $\sqrt{R_{eff}P} = V_C$, we can calculate t_c, which can be expressed as

$$t_c = -\frac{R_{eff}C}{2}\ln\left[R_{eff}P\left(1 - 0.95^2\right)\right] - t_1 \tag{9}$$

Moreover, based on the above discussion, we can obtain the formula for V_{C0}, which can be expressed as

$$V_{C0} = \min\left(\sqrt{R_{eff}P}, V_S\right) \tag{10}$$

Equation (10) is capable of describing V_{C0} before and after γ-ray exposures.

With (8)-(10), we can calculate the dose dependence of t_c and V_{C0} as presented in Fig. 10 and 11. Overlaid on the data in the two figures is the close agreement of the experimental data with (8)-(10).

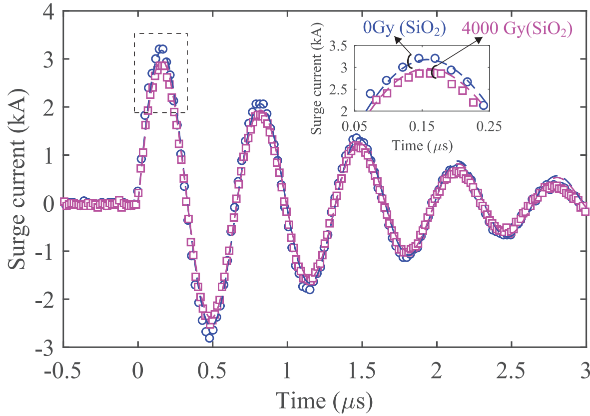

FIGURE 12. Surging current waves of PDC before and after γ-ray exposures. The markers are experimental results, and the dash lines are calculated results by (12). The inset shows data in the dotted box.

VI. DAMAGE ON DISCHARGING CHARACTERISTICS

A. EXPERIMENTAL RESULTS

Fig. 12 displays the variations in the surging current waves (I_D) of PDCs before and after the γ-ray irradiation. After a relative high dose exposure, 4000 Gy(SiO_2), the peak surge current (I_{peak}) decreases by ~6%. For the cases of lower dose (less than ~3000 Gy(SiO_2)) and higher dose (larger than ~5000 Gy(SiO_2)), I_D is almost unchanged, and both the two situations are not plotted in this work. As stated in the following Section VI-B, the discharge behaviours of PDC can be modelled by a resistor-inductor-capacitor circuit in under-damping state. I_D behaves a resonant wave with decreasing amplitude, and its resonant frequency is almost unchanged for dose up to 9160 Gy(SiO_2) as presented in Fig. 12.

B. MODELLING

The AS-MCT in on-state is immune to TID damage, and can be behaviorally modeled as a resistor as stated in Section IV-A. Then, we can figure out the equivalent circuit for PDC in discharging as presented in Fig. 13. It is obviously that the discharging behaviours of PDC are controlled by its equivalent resistor-inductor-capacitor circuit. During test, the AS-MCT and high voltage probe are in parallel. As the on-state resistance of AS-MCT (mΩ) is smaller than that of high voltage probe (MΩ) with several orders, the influence of high voltage probe on surge behaviour can be omitted.

The voltage within the discharge loop is convergent, which can be expressed as

$$\frac{dV_C}{dt}+\frac{dV_R}{dt}+\frac{dV_L}{dt}=L\frac{d^2I_D}{dt^2}+R\frac{dI_D}{dt}+\frac{1}{C}I_D=0 \quad (11)$$

The parameters are defined in Table 1 (Section III-A). With the initial conditions of $I_D(t=0)=0$ and $V_C(t=0)=V_{C0}$, we can obtain the solution to (11), which takes the form as

$$I_D(t)=\frac{V_{C0}}{\omega L}\exp\left(\frac{Rt}{2L}\right)\sin(\omega t) \quad (12)$$

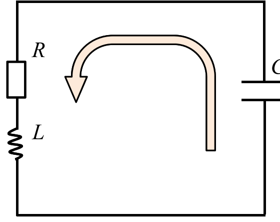

FIGURE 13. Simplified equivalent circuit for the discharging process of PDC.

where ω is the resonant frequency of surge current which can be expressed as

$$\omega=\sqrt{\frac{1}{LC}-\left(\frac{R}{2L}\right)^2} \quad (13)$$

The peak surge current (I_{peak}) occurs at the end of the first quarter period, i.e., $t=1/4\omega$. Thus, with (12), I_{peak} can be expressed as

$$I_{peak}=\frac{2V_{C0}}{\sqrt{4L^2/C^2-R^2}}\exp\left(\frac{R\pi}{2\sqrt{4L^2/C^2-R^2}}\right) \quad (14)$$

Fig. 13 indicates that I_{peak} and ω are 3.2 kA and 9.5 MHz respectively for PDC switched by un-irradiated AS-MCT. The parasitic resistance (R) and inductance (L) of our test PDC can be calculated by (13) and (14) which are listed in Table 1. For PDC in discharge stage, the on-state resistance of AS-MCT dominates R. The on-state resistance weakly depends on I_D. A higher I_D means larger carrier concentrations in A-MCT which produces a smaller on-state resistance. Thus, R for surge currents (39 mΩ), hundreds of A, is smaller than the AS-MCT on-state resistance obtained in Fig. 4 for relative small currents (65 mΩ), tens of A. Nevertheless, the two extracted resistances coincide with each other which confirms that the AS-MCT in surge applications approximately behaves as a resistor of small value.

C. DAMAGE MECHANISMS

Equation (13) shows that the resonant frequency (ω) of surge current is determined by R, L and C. R is dominated by the AS-MCT on-state resistance. The AS-MCT on-state resistance is intrinsically immune to γ-ray exposures (Section IV-A), and thus R is almost unchanged following high dose exposures. L mainly originates from the electrode and package of devices which is insensitive to γ-ray exposures. The capacitor is not exposure to γ-ray, and C is a constant. Thus, ω is almost unchanged even after high dose exposures as presented in Fig. 12.

The initial capacitor voltage (V_{C0}) is previously determined by (10). Substituting the parameters in Table 1 and V_{C0} into (12), we can reproduce the oscillation waves of I_D before and after γ-ray exposures as presented in Fig. 12. Overlaid on the data in Fig. 12 is the close agreement of the experimental data with (12). Fig. 12 shows I_{peak} exhibits

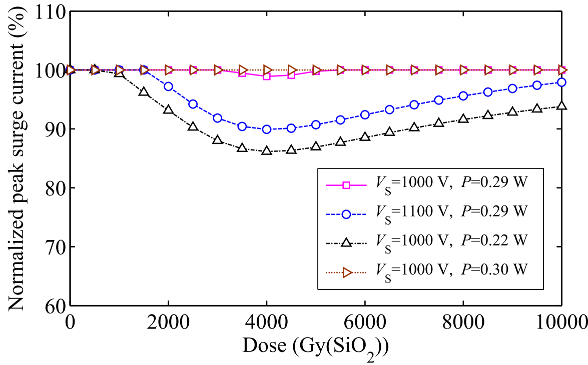

FIGURE 14. Dose dependence of peak surge current at various circuit conditions obtained by (10) and (14). In figure, *P* and V_L are the power and voltage limitations of charging source.

TID sensitivity. Equation (14) indicates a linear dependence of I_{peak} on V_{C0}. Thus, the TID response of I_{peak} can be explained by that of V_{C0} as presented in Fig. 11. For the case of low dose, up to ∼3000 Gy(SiO_2), I_{peak} is almost unchanged as there is no significant TID damage on V_{C0}. After middle dose exposures, ∼3000-5000 Gy(SiO_2), V_{C0}, and thus I_{peak}, decreases by a few percent. With a further increase of dose, both V_{C0} and I_{peak} are retorted to their initial values.

VII. DISCUSSION

A. CHARING TIME AND PEAK CURRENT

The charing time (t_c in Section V-C) and peak surging current (I_{peak} in Section VI-B) are key parameters for PDC. t_c confines the minimum time interval between charge and discharge stages, and is important to the timing of PDC. I_{peak} can be used to characterize the energy transmission efficiency of PDC. In this section, we discuss the TID response of t_c and I_{peak} on circuit parameters.

After TID exposures, the decrease of leakage current resistance of AS-MCT (R_{MCT} in Section IV-B) accounts for the degradations of t_c and I_{peak}. As R_{MCT} shows a "tick"-like dependence on γ-ray dose (see Fig. 7), the degradations of t_c and I_{peak} are recoverable after high dose exposures (Sections V-C and VI-C). Equation (8) shows that the TID damage of t_c is inevitable, and t_c can increase several times when the dose is up to thousands of Gy(SiO_2). Fig. 14 presents the influence of the power (P) and voltage (V_L) limitations of charging source on the TID response of I_{peak}. A smaller P and higher V_L can aggravate the TID damage on I_{peak}. For the cases of $V_L = 1000$ V and $P = 0.22$ W, the degradation of I_{peak} can be significant and up to 15% following 4000 Gy(SiO_2) exposure. In this work, an extra equipment (PS350 power source) is adopted to charge the capacitor. This condition is not realistic in missions. Under such conditions, the capacitor will be charged by an integrated power source with small P, such as 0.2 W. Thereafter, the TID-induced damage on I_{peak} can be a serious problem. And, the radiation hardness for I_{peak} should be considered.

B. RADIATION HARDNESS

We define that $t_{c\text{-}max}$ is the maximum acceptable value of charging time for PDC following TID exposures. The criterion R_{MCT} ($R_{MCT\text{-}tc}$) corresponding to $t_{c\text{-}max}$ can be calculated by (8) under the constraint of $t_c(R_{MCT\text{-}tc}) = t_{c\text{-}max}$, i.e.,

$$t_{c\text{-}max} = -\frac{R_{MCT\text{-}tc}R_P C}{2(R_{MCT\text{-}tc} + R_P)}\ln\left(\frac{R_{MCT\text{-}tc}R_P P}{R_{MCT\text{-}tc} + R_P} - V_L^2\right) - t_1 \quad (15)$$

The TID damage of I_{peak} can be eliminated. The minimum value of R_{MCT} ($R_{MCT\text{-}p}$), which makes I_{peak} immune to ionization damage, can be figured out by (3), (10) and (14) under the constraint of $I_{peak}(\min(R_{eff})) = I_{peak}(R_{eff} = \infty)$. Then, $R_{MCT\text{-}p}$ can be expressed as

$$\frac{R_{MCT\text{-}p}R_P}{R_{MCT\text{-}p} + R_P} = \frac{V_L^2}{P} \quad (16)$$

For a radiation hardened PDC, both (15) and (16) should be satisfied. The radiation hardness criterion can be expressed as

$$\min(R_{MCT}) \geq \min\left(R_{MCT\text{-}tc}, R_{MCT\text{-}p}\right) \quad (17)$$

Equation (17) limits the minimum R_{MCT} for AS-MCT switch of PDCs in radiation environments. The TID-induced leakage current in AS-MCT (I_{MCT}) accounts for the decrease of R_{MCT}. The techniques, which can alleviate the increase in I_{MCT}, can improve the radiation harness of I_{peak}. Up to now, I_{MCT} is not well modelled, and thus, the radiation hardness of I_{peak} will be discussed in a further work.

VIII. CONCLUSION

The AS-MCT, a composite structure of metal-oxide-silicon and bipolar junction transistors, is susceptible to TID. In pulse discharge circuit, the AS-MCT switch behaves as resistors in both charge and discharge stages. After TID exposures, the equivalent leakage-current-resistance of AS-MCT in open-gate forwarding blocking mode (R_{MCT}) decreases as the leakage current increases. Thereafter, the degradation of R_{MCT} effectuates the increase in charging time (t_c) and decrease in peak surge current (I_{peak}) of short pulse discharge circuit. As R_{MCT} show a "tick"-like dependence on the γ-ray dose, the TID damage of t_s and I_{peak} are recoverable after high dose exposures, thousands of Gy(SiO_2). For pulse discharge circuit, small capacitor voltage and large charging power can improve the degradation of I_{peak} induced by the TID damage of AS-MCT switch.

REFERENCES

[1] L. Li *et al.*, "Experimental study on displacement damage effects of anode-short MOS-controlled thyristor," *IEEE Trans. Nucl. Sci.*, vol. 67, no. 3, pp. 508–517, Apr. 2020.

[2] L. Li *et al.*, "A study on ionization damage effects of anode-short MOS-controlled thyristor," *IEEE Trans. Nucl. Sci.*, vol. 67, no. 9, pp. 2062–2072, Sep. 2020.

[3] W. J. Chen *et al.*, "High peak current MOS gate-triggered thyristor with fast turn-on characteristics for solid-state closing switch applications," *IEEE Electron Device Lett.*, vol. 37, no. 2, pp. 205–208, Feb. 2016.

[4] W. J. Chen *et al.*, "A behavioral model for MCT surge current analysis in pulse discharge," *Solid-State Electron.*, vol. 99, pp. 31–37, Sep. 2014.

[5] W. J. Chen *et al.*, "Non-simultaneous triggering induced failure of CS-MCT under repetitive high-current pulse condition," *IEEE Trans. Device Mater. Rel.*, vol. 20, no. 1, pp. 214–220, Mar. 2020.

[6] C. Xu, P. Zhu, K. Chen, W. Zhang, R. Q. Shen, and Y. H. Ye, "A highly integrated conjoined single shot switch and exploding foil initiator chip based on MEMS technology," *IEEE Electron Device Lett.*, vol. 38, no. 11, pp. 1610–1613, Nov. 2017.

[7] H. Wang *et al.*, "Investigation on switching energy losses in reversely switched dynistor," *IEEE Trans. Power Electron.*, vol. 29, no. 4, pp. 1553–1556, Apr. 2014.

[8] E. V. Chernyavskii, V. P. Popov, Y. S. Pakhmutov, and L. N. Safronov, "MOS-controlled thyristor: A study of a promising power-switching device," *Russian Microelectron.*, vol. 31, no. 5, pp. 376–381, 2002.

[9] J. R. Srour and J. W. Palko, "Displacement damage effects in irradiated semiconductor devices," *IEEE Trans. Nucl. Sci.*, vol. 60, no. 3, pp. 1740–1766, Jun. 2013.

[10] D. M. Fleetwood, "Total ionizing dose effects in MOS and low-dose-rate-sensitive linear-bipolar devices," *IEEE Trans. Nucl. Sci.*, vol. 60, no. 3, pp. 1706–1730, Jun. 2013.

[11] D. M. Fleetwood, L. C. Riewe, J. R. Schwank, S. C. Witczak, and R. D. Schrimpf, "Radiation effects at low electric fields in thermal, simos, and bipolar-base oxides," *Appl. Phys. Lett.*, vol. 43, no. 6, pp. 2537–2546, Dec. 1996.

[12] I. S. Esqueda, H. J. Barnaby, K. E. Holbert, and Y. Boulghassoul, "Modeling inter-device leakage in 90 nm bulk CMOS devices," *IEEE Trans. Nucl. Sci.*, vol. 58, no. 3, pp. 793–799, Jun. 2011.

[13] L. Li *et al.*, "Improved model for ionization-induced surface recombination current in PNP BJTs," *IEEE Trans. Nucl. Sci.*, vol. 67, no. 8, pp. 1826–1834, Aug. 2020.

[14] L. Li *et al.*, "Current gain degradation model of displacement damage for drift BJTs," *IEEE Trans. Nucl. Sci.*, vol. 66, no. 4, pp. 716–723, Apr. 2019.

[15] X. J. Li *et al.*, "Characteristic of displacement defects in n-p-n transistors caused by various heavy ion irradiations," *IEEE Trans. Nucl. Sci.*, vol. 64, no. 3, pp. 976–982, Mar. 2017.

[16] J. Q. Yang, X. J. Li, C. M. Liu, and D. M. Fleetwood, "The effect of ionization and displacement damage on minority carrier lifetime," *Microelectron. Rel.*, vol. 82, pp. 124–129, Mar. 2018.

[17] D. H. Loescher, W. R. Dawes, and D. B. King, "Co-60 and neutron irradiation of MOS-controlled thyristors," *IEEE Trans. Nucl. Sci.*, vol. 36, no. 6, pp. 2411–2414, Dec. 1989.

[18] C. Xu, P. Zhu, W. Zhang, R. Q. Shen, and Y. H. Ye, "A plasma switch induced by electroexplosion of p-n junction for mini exploding foil initiator," *IEEE Trans. Plasma Sci.*, vol. 47, no. 5, pp. 2710–2716, May 2019.

[19] B. J. Baliga, *Fundamentals of Power Semiconductor Devices*. New York, NY, USA: Springer, 2008, pp. 203–277.